Rheologica Acta (2023) 62:129–143
https://doi.org/10.1007/s00397-023-01383-2

ORIGINAL CONTRIBUTION

Experimental and simulative determination and correction of the effective gap extension in structured coaxial measuring systems

Sebastian Josch[1] · Steffen Jesinghausen[1] · Christopher Dechert[2] · Hans-Joachim Schmid[1]

Received: 11 October 2022 / Revised: 29 December 2022 / Accepted: 4 January 2023 / Published online: 16 January 2023

Abstract

The use of structured measuring systems to prevent wall slip is a common approach to obtain absolute rheological values. Typically, only the minimum distance between the measuring surfaces is used for further calculation, implying that no flow occurs between the structural elements. But this assumption is misleading, and a gap correction is necessary. To determine the radius correction Δr for specific geometries, we conducted investigations on three Newtonian fluids (two silicon oils and one suspension considered to be Newtonian in the relevant shear rate range). The results show that Δr is not only shear- and material-independent, but geometry-dependent, providing a Newtonian flow behaviour in a similar viscosity range. Therefore, a correction value can be determined with only minute deviations in different Newtonian fluids. As the conducted laboratory measurements are very time-consuming and expensive, a CFD-approach with only very small deviations was additionally developed and compared for validation purposes. Therefore, simulation is an effective and resource-efficient alternative to the presented laboratory measurements to determine Δr for the correction of structured coaxial geometries even for non-Newtonian fluids in the future.

Keywords Wall slip prevention · Effective gap extension · Structured geometries · Coaxial system · Correction · Simulation

Introduction

One fundamental issue while measuring rheological properties of complex materials is wall slip (e.g. for suspensions). In general, the presence of wall slip leads to an underestimation of the actual viscosity, which can, for example, not only lead to an incorrect design of production plants, but also create considerable problems in the field of simulation, where the viscosity often serves as an input parameter. Wall slip is characterized by a jump in velocity directly at the wall, i.e. true wall slip or strongly increasing velocity gradient in close proximity to the wall, i.e. apparent wall slip (Pahl et al. 1991). However, true wall slip is rarely observed in reality (Haase et al. 2017), since all surfaces show a certain roughness at the atomic level (Zhu and Granick 2002; Granick et al. 2003). Therefore, the term wall slip will be used in the following as a synonym for apparent wall slip.

The reason for wall slip is the development of a thin slipping layer σ directly at the wall, with a much lower viscosity compared to the bulk material (see Fig. 1a). This is especially prominent for suspension flows, since a particle depleted area with a strongly reduced viscosity occurs at the wall (Banfill 1991; Macosko 1994; Barnes 1995; Jesinghausen et al. 2016). Several phenomena lead to these low particle concentrations, with geometric constraint, i.e. the particles cannot penetrate the wall, being probably the most important. For monodisperse, spherical particles the typical size range of the slipping layer σ is in the range of the particle radius (Yilmazer and Kalyon 1989; Kalyon 2005; Ballesta et al. 2012; Jesinghausen et al. 2016). Other relevant mechanisms include particle migration due to gradients in shear rate, repulsive particle–wall-interactions and particle layering on surfaces caused by the flow (Besseling et al. 2010; Korhonen et al. 2015; Cloitre and Bonnecaze 2017).

Since the correction of wall slip always requires different sets of coaxial measurement geometries and in general a high measuring effort (Mooney 1931; Yoshimura et al. 1988; Kiljański 1989), the prevention of wall slip by roughened or

✉ Steffen Jesinghausen
Steffen.jesinghausen@upb.de

[1] Particle Technology Group, Paderborn University, Paderborn, Germany

[2] Fluid Process Engineering, Paderborn University, Paderborn, Germany

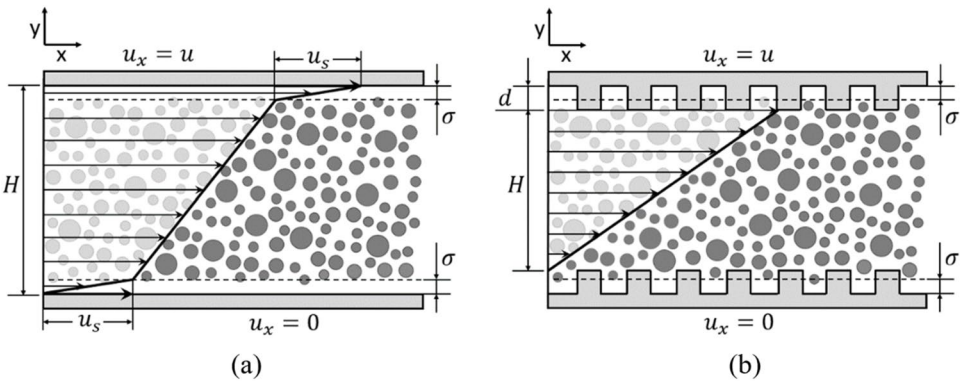

Fig. 1 **a** Schematic illustration of the velocity profile in the two-plate-model with the velocity of the upper plate u_x, the slip velocity u_s, the gap width H, the structure depth d and the slip-layer or particle depleted area σ; **b** prevention of wall slip through profiled measuring surfaces with new defined gap height H

rather structured geometries is usually practiced (Pawelczyk et al. 2020). In this case, the tip-to-tip distance H between the surfaces defines the measuring gap for further calculation (see Fig. 1b). The use of such geometries does not prevent the particle-depleted layer, but it shifts it to a region that is not relevant to the essential flow field. However, the assumption of a distinct flow-interface at the geometry tips is void, as various investigations revealed, and leads to calculation errors (Pawelczyk et al. 2020).

Fincke and Heinz (1961) conducted research on the determination of yield stress of coarse suspensions by using grooved coaxial measuring geometries for wall slip prevention. In order to determine, if the material located in the grooves participates in the shear flow or not, they measured Newtonian fluids with these geometries. The results have shown that the effective radius differs from the true radius by a few tenths of a millimetre. After applying these correction values to the calculation of a Newtonian oil, no deviations between smooth and grooved measuring system could be observed. Since the effective radius and the actual radius do not differ that much, the authors state that the flow penetration depth in the grooves is only small. However, according to Fincke and Heinz, this is dependent of the fluid behaviour and the applied shear stress. Bauer et al. (Bauer et al. 1995), who investigated concentrated diblock copolymer solutions in grooved coaxial systems, determined the correction values in advance by measuring several Newtonian fluids. The correction value ΔR was found to be proportional to the radius R but independent of viscosity and shear rate. With these corrected radii, they were able to obtain the same results for smooth and grooved measuring geometries, even for non-Newtonian fluids. However, they state that while the correction factors can be used to include the influence of the grooved surface, they do not consider the disturbance of the flow field. This is particularly important when measuring materials that exhibit a shear-dependent build-up of structures that leads to shear-thickening behaviour. Since a structured geometry can cause this behaviour at a lower shear rate than a smooth geometry, a wrong interpretation of the flow behaviour could be possible. Similar results were obtained by Ahuja et al. (Ahuja and Singh 2009), who compared simulated viscosity values of smooth and serrated geometries for low concentrated suspensions. When using the tip-to-tip distance in the simulation, deviations between smooth and serrated walls occurred. However, when simulating the serrated walls with the actual gap, i.e. tip-to-tip distance H plus two times the serration-depth, the deviations vanished, indicating a significant flow in the serration.

Besides the mentioned investigations concerning coaxial systems, various research on parallel-plate systems were conducted. However, as this paper focuses on coaxial systems, other measuring geometries will not be discussed in detail. Information on the investigations concerning these systems and the underlying theoretical backgrounds can be found in (Beavers and Joseph 1967; Neale and Nader 1974; Nickerson and Kornfield 2005; Carotenuto and Minale 2013; Minale 2014, 2016; Carotenuto et al. 2015; Paduano et al. 2018, 2019; Pawelczyk et al. 2020).

The presented studies clearly show that the application of structured geometries in coaxial systems leads to an increase in the effective radius and to the need for radius corrections to determine correct rheological values. However, for materials prone to wall slip, such as suspensions, those geometries are widely used and partially irreplaceable, but often without the necessary correction. In order to develop a simple method for determining the radius correction of any geometry, we conducted investigations on two homogeneous Newtonian fluids and a medium dense suspension comparing laboratory measurements and CFD for various kinds of coaxial measuring geometries, primarily differing in groove widths and depths. In a first step, correction values for the radii, which can be seen as theoretical penetration depths, were derived via experimental comparison of structured geometries to smooth geometries for the Newtonian fluids. Second, as this would surely simplify future investigations, a CFD simulation was built to determine the correction values, which shows a strong agreement to the experiments. At last, the results were transferred to a medium dense suspension and the applicability is demonstrated.

Material and methods

Theoretical background

Concentric cylinder measuring systems consist of two cylinders with the same symmetry axis. The material is sheared in a gap between the inner cylinder (bob, radius r_i and length L) and the outer cylinder (cup, radius r_o and length L). Since the surface area of the cylindrical plane increases from $r = r_i$ to $r = r_o$, the shear stress occurring in the measuring gap decreases with increasing radius r (see Eq. (1)). If dealing with a Newtonian fluid, the shear rate can be expressed through Eq. (2), where ω_i and ω_o are the angular velocity at the inner or outer cylinder, respectively, and $\beta = (r_i/r_o)^2$ (Pahl et al. 1991; Mezger 2012).

$$\tau(r) = M/(2 \bullet \pi \bullet r^2 \bullet L) \tag{1}$$

$$\dot{\gamma}(r) = \frac{2 \bullet r_i^2 \bullet (\omega_i - \omega_o)}{r^2 \bullet (1 - \beta)} \tag{2}$$

For a Searle type cylinder system, which was used in this paper, only the inner cylinder is rotating. Thus, $\omega_o = 0$ and the viscosity for a Newtonian fluid can be expressed as shown in Eq. (3) (Pahl et al. 1991; Mezger 2012).

$$\eta = \frac{M \bullet (1 - \beta)}{4 \bullet \pi \bullet \omega_i \bullet r_i^2 \bullet L} \tag{3}$$

Usually, the flow behaviour of the sample is not known or rather non-Newtonian and, therefore, the calculation according to Eqs. (1) to (3) is not applicable anymore. To this end, an approximation method using the so-called representative shear rate $\dot{\gamma}_{rep}$ and representative shear stress τ_{rep} is commonly applied, as it is fast and simple even though better, but more complicated correction methods exist (Krieger and Elrod 1953; Giesekus and Langer 1977). Schümmer (Schümmer 1970) showed that for any fluid a representative radius r_{rep} exists, where the shear rate and the shear stress are equal to those of a Newtonian fluid. Based on that, Giesekus and Langer (Giesekus and Langer 1977) developed equations for the shear rate $\dot{\gamma}_{rep}$ and shear stress τ_{rep}, which are independent of the flow behaviour (see Eqs. (4) and (5)). It is to mention that the factor ε originates from a series expansion, with usually only the first series element to be used for further calculation, as for narrow gaps $(1 - \beta \ll 1)$ the deviation is negligibly small.

$$\dot{\gamma}_{rep} = \frac{1 + \beta}{2} \cdot \dot{\gamma}_i = \varepsilon \cdot \dot{\gamma}_i \tag{4}$$

$$\tau_{rep} = \frac{1 + \beta}{2} \cdot \tau_{i} = \varepsilon \cdot \tau_i \tag{5}$$

Since this approximation is implemented in the evaluation method for the concentric cylinder measuring systems of the rheometer used in this paper, the expressions τ and $\dot{\gamma}$ will generally refer to the above-mentioned representative values. However, the viscosity remains independent of whether the representative values were used for the shear stress and the shear rate because the factor ε is truncated in the viscosity calculation.

Wall slip correction

The fundamental issue with wall slip is that the wall slip velocity u_s leads to an apparent shear rate $\dot{\gamma}_a$, which is always higher than the true shear rate $\dot{\gamma}$ applied to the material. Thus, the obtained viscosity is lower than the true viscosity. To overcome this, Yoshimura and Prud'homme developed a correction method for coaxial systems, which allows for the determination of true shear rate and true viscosity (Yoshimura et al. 1988).

As the correction method is based on the use of two gaps and coaxial systems generally have a fixed gap width, the use of two systems with different radii is necessary. According to Yoshimura and Prud'homme (Yoshimura et al. 1988), the ratio κ between outer and inner radii has to be the same for both systems (see Eq. (6)).

$$\frac{r_{o,1}}{r_{i,1}} = \frac{r_{o,2}}{r_{i,2}} = \kappa \tag{6}$$

Adjusting equal shear stresses for both systems, the angular velocity can then be expressed by:

$$\omega_1 = \omega_{s,1} + \omega_f = \frac{1}{r_1} \bullet \left(\frac{u_s(\tau_o)}{\kappa} + u_s(\tau_i) \right) + \int_{\tau_o}^{\tau_i} \frac{\dot{\gamma}(\tau)}{2 \bullet \tau} d\tau \tag{7}$$

$$\omega_2 = \omega_{s,2} + \omega_f = \frac{1}{r_2} \bullet \left(\frac{u_s(\tau_o)}{\kappa} + u_s(\tau_i) \right) + \int_{\tau_o}^{\tau_i} \frac{\dot{\gamma}(\tau)}{2 \bullet \tau} d\tau \tag{8}$$

Since the fluid angular velocity term ω_f is equal for both systems, and the slip velocities are a function of stress only, which results in equal bracketed terms, Eqs. (7) and (8) can be simplified and combined to calculate ω_f,according to Eq. (9).

$$\omega_f = \frac{r_2 \bullet \omega_2 - r_1 \bullet \omega_1}{r_2 - r_1} \tag{9}$$

With regard to the representative shear stress τ_{rep} shown in Eq. (5), it can also be expressed by:

$$\tau_{rep} = \frac{M}{4 \bullet \pi \bullet L \bullet r_i^2} \bullet \left(\frac{\kappa^2 + 1}{\kappa^2} \right) \tag{10}$$

The true viscosity can then be calculated by:

$$\eta = \frac{\tau_{rep}}{\omega_f} \bullet \left(\frac{\kappa^2 - 1}{\kappa^2 + 1} \right) \tag{11}$$

Geometries

The reference system used in this investigation was a smooth concentric cylinder (CC) system (Anton Paar CC27) with an inner radius $r_i = 13.333$mm, an outer radius $r_o = 14.462$mm and a measuring length $L = 40.026$mm. For wall slip correction, two other coaxial systems called CC14 and CC25 were manufactured (see Table 1). Both systems fulfil the requirements of the ISO 3219 for standardized systems. In order to determine the influence of structural parameters on the effective gap size, further structured coaxial systems were developed based on the CC25-system (see Fig. 2a). Three different groove depths ($d_1 = 0.3$mm, $d_2 = 0.65$mm, $d_3 = 1$mm) and two different groove widths ($w_1 = 1.1$mm (narrow), $w_2 = 2.1$mm (wide)) were analysed, while the groove shape is always rectangular. The measuring length of the inner cylinder of all systems is $L = 36.84$mm. Concerning the groove depths, it is to mention that due to the rectangular shape combined with the curved surface of the cylinders, the depth of a groove is always the largest depth possible when referring to the outer or inner radius, respectively. This leads to the inner cylinder having the maximum groove depth in the middle of a groove, while the outer cylinder having the maximum groove depth at the edge of a groove (see Fig. 2b). The systems were 3D-printed out of stainless steel with a small oversize and then reworked on a lathe to ensure the dimensional accuracy. The individual dimensions can be found in Table 1, where the corresponding geometries and dimensions are given in the form "*rdddw*" (*r* = rectangular, *ddd* = groove depth in 10µm, *w* = groove width in rounded mm).

Table 1 Geometric dimensions of the manufactured coaxial systems

Measuring system	r_i/mm	r_o/mm	L/mm	d/mm	w/mm
CC14	7.080	7.680	21.240	-	-
CC25	12.280	13.320	36.840	-	-
CC27 (Anton Paar)	13.333	14.462	40.026	-	-
r0301	12.265	13.305	36.840	0.30	1.1
r0651	12.270	13.310	36.840	0.65	1.1
r1001	12.260	13.295	36.840	1.00	1.1
r0302	12.260	13.295	36.840	0.30	2.1
r0652	12.260	13.295	36.840	0.65	2.1
r1002	12.260	13.305	36.840	1.00	2.1

Laboratory measurements

All measurements were conducted using a Physica MCR 501 rheometer from Anton Paar. Since it is possible to temper coaxial systems quite efficiently, the mean temperature of all measurements was within $T = 20.0 \pm 0.01$°C. The rheometer has a maximum torque accuracy of 0.5%, which equals 0.2µNm. For the fluids measured in this paper with AK 1000 being the one with the lowest viscosity, a shear rate of $0.1s^1$ results in a torque error of about 5%, which reduces to only 0.4% at $1s^1$. For rheometre controlling and data acquisition, the Anton Paar software "RheoPlus" (RHEOPLUS/32 V3.31) was used.

The materials analysed in this investigation were Wacker AK 1000 and AK 5000 silicon oils, which have a kinematic viscosity of $\nu = 1000\text{mm}^2/\text{s}$ and $\nu = 5000\text{mm}^2/\text{s}$, respectively (manufacturer specification) and show a nice Newtonian behaviour in the examined shear rate range (see Fig. 3). The AK 5000 was also used to prepare a suspension together with 21.23vol% Spheromers® CA40 particles ($x_{50,3} = 48.5$µm measured with *Sympatec QICPIC*).

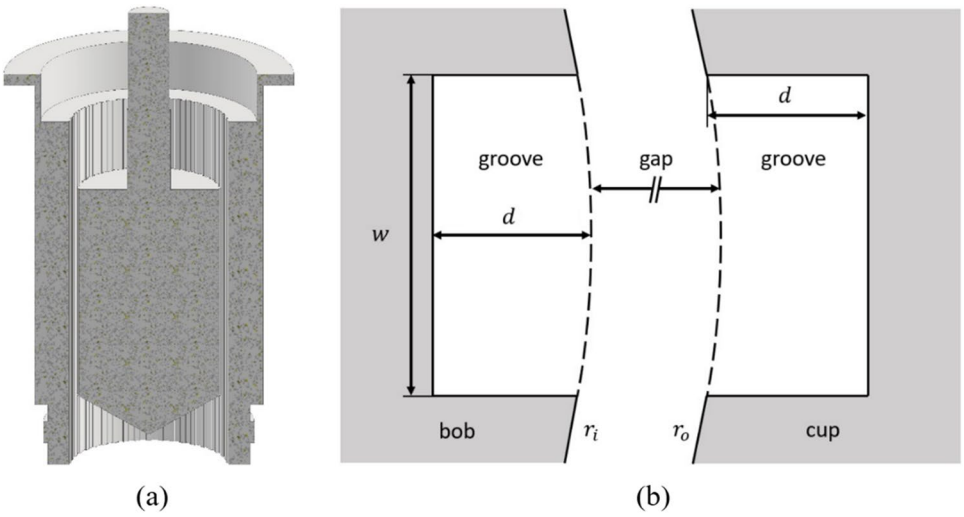

Fig. 2 **a** CAD-construction of a grooved measuring system; **b** schematic illustration of the groove and gap dimensions

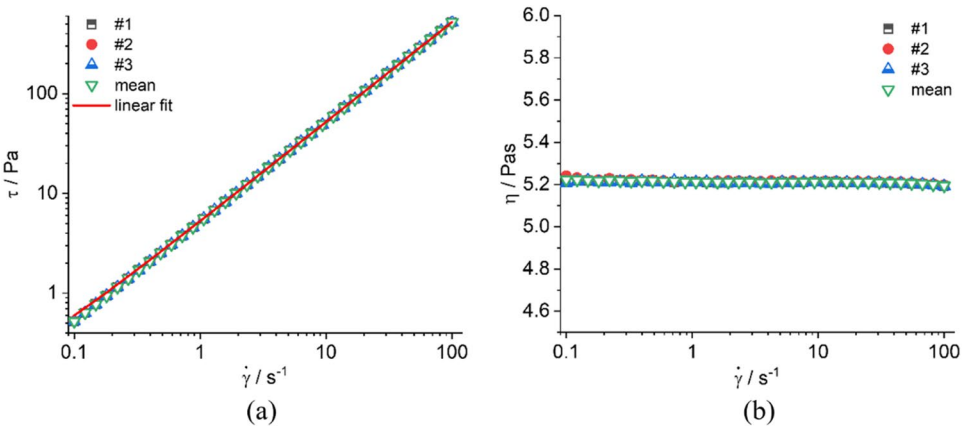

Fig. 3 Individual measurements #1–#3 and mean value for silicon oil AK 5000 measured with CC27 system at $T = 20.0 \pm 0.01$°C; **a** shear stress over shear rate; **b** viscosity over shear rate

Table 2 Measuring program

Tempering time/min	10(silicon oil)/15 (suspension)
Duration pre-shearing/s	30
Shear rate pre-shearing/s^1	10
Pause/*s*	15
Log. Shear rate ramp/s^1	0.1 – 100
Number of measuring steps/–	36
Log. Measuring time/s	10 – 5

As silicon oils are a very homogeneous material, no premeasurement treatment was necessary. The suspensions, however, were prepared individually before every measurement procedure, which consists of three single measurements, by mixing the right amount of particles with the silicon oil. This was done to ensure the reproducibility by preventing variations in concentration due to inhomogeneities, which could have developed over time, even though that would have been very unlikely. After mixing the suspensions, they were degassed in an ultrasonic bath at 19°C for 1 h and then mixed again. As the suspensions heated up to 30°C due to internal friction, they were cooled to a target temperature of 20°C with constant stirring in a water bath before pouring them into the measuring cup.

In order to prevent the formation of air bubbles, the materials were carefully poured along the wall of the geometries. Subsequently, the measuring bob was lowered very slowly (100µm/s) into the cup and the temperature was set to 20°C. After excess material was removed or additional material was filled into the measuring gap, the measuring program was started (see Table 2).

For an easier comparison, the measured (apparent) viscosity values of the structured geometries η_a are normalized at each shear rate according to the reference viscosity η_{CC27} and are labelled η_n, as depicted in Eq. (12).

$$\eta_n = \frac{\eta_a}{\eta_{CC27}} \tag{12}$$

Simulation

CFD simulations were conducted using the open source software OpenFOAM (version v2012). The STL-files for the geometry were compiled using the freeware Blender and meshed via the blockMesh- and snappyHexMesh-tool of OpenFOAM. Since the flow field in the measuring gap can be described two-dimensional within a reasonable error margin, the virtual measuring gap was designed with a length of 0.3mm for easier meshing and further simulated in 2D using the solver simpleFoam. For further analysis of the flow field, a customized solver was developed, whose functionality is explained in "Simulation results — investigation of the penetration depth and the flow field via simulation".

Even though this is basically a dynamic simulation, there is only interest in the steady-state flow field. Therefore, the so-called MRF (multiple reference frame) method was used, which works with a stationary mesh, but still considers the rotation by adjusting the momentum equation. Additional geometries were constructed describing the rotating zone, whose outer radius is equal to $(r_i + r_o)/2$ of the geometry in question.

The post-processing and extracting of individual cell values was done via the freeware ParaView. Combined with a self-written MATLAB algorithm, a profound evaluation of the flow field and the penetration depths was possible.

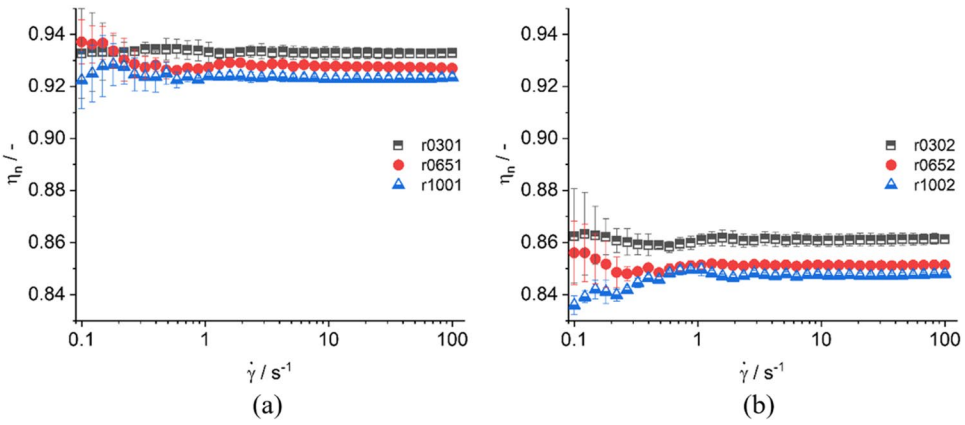

Fig. 4 Normalized viscosity η_n over the shear rate $\dot{\gamma}$ for silicon oil AK 5000 calculated for narrow groves (**a**) and wide grooves (**b**)

Determination of correction values

The idea behind the correction is that a general radius correction value Δr can be derived for individual measuring systems and applied to a huge variety of materials. Based on the correction method presented for parallel plate systems (Nickerson and Kornfield 2005), we developed a method to determine the radius correction in coaxial systems. However, some assumptions need to be made for applying this correction.

If there was no influence of the structured measuring surfaces, meaning the interface of the flow field is indeed the tip-to-tip-distance, the same viscosity must be measured using the structured geometries and the CC27 reference system. As this is clearly not the case, a correction is necessary. The approach for the correction is that the true viscosity η_{true}, which has to be equal to the reference viscosity η_{CC27}, can be calculated from the apparent viscosity η_a, which is measured with the structured systems, by implementing a correction radius Δr. This correction value needs to be included both for the inner radius Δr_i and the outer radius Δr_o. However, to guarantee a stable numerical solution method, the assumption $\Delta r_i = \Delta r_o = \Delta r$ has to be made. Therefore, based on Eq. (3) by truncating all equal parameters except $\beta = (r_i/r_a)^2$ and r_i, which differ because of the Δr, the following relation between η_{true} and η_a can be derived (see Eq. (13)). As η_{true} and η_a as well as r_i and r_o are known, the radius correction Δr can be easily calculated. To apply the radius correction, η_{true} and η_a need to be corrected for their flow behaviour a priori. Therefore, it can be assumed that Eq. (13) is not only valid for Newtonian fluids. Corresponding application to shear-thinning fluids can be found in (Pawelczyk et al. 2020).

$$\frac{\eta_{true}}{\eta_a} = \frac{\frac{M\bullet(1-\beta_{true})}{4\bullet\pi\bullet\omega_i\bullet(r_i-\Delta r_i)^2\bullet L}}{\frac{M\bullet(1-\beta)}{4\bullet\pi\bullet\omega_i\bullet r_i^2\bullet L}} = \frac{\left(1-\frac{(r_i-\Delta r_i)^2}{(r_o+\Delta r_o)^2}\right)\cdot r_i^2}{\left(1-\frac{r_i^2}{r_o^2}\right)\cdot(r_i-\Delta r_i)^2} = \frac{\left(1-\frac{(r_i-\Delta r)^2}{(r_o+\Delta r)^2}\right)\cdot r_i^2}{\left(1-\frac{r_i^2}{r_o^2}\right)\cdot(r_i-\Delta r)^2} \tag{13}$$

Table 3 Parameters of the linear regressions for AK 1000, AK 5000 and the suspension

Material	η/Pa · s	R^2
AK 1000	1.087 ± 0.003	≈ 1
AK 5000	5.211 ± 0.001	≈ 1
Suspension	11.369 ± 0.017	≈ 1

Results and discussion

The following chapters address separately the results obtained during the laboratory measurements and the simulation. The main focus of the laboratory results is to determine the radius corrections by comparing the values measured with the structured geometries with the reference values, applying these corrections and transferring them to another homogeneous Newtonian fluid. The simulation results focus firstly on the evaluation of the simulation method and then a comparison between simulation and laboratory results will be conducted, followed by the transfer to suspensions.

Laboratory results

In order to obtain reference values, the silicon oils were measured with the standard geometry CC27. Since a wall slip correction needs to be conducted for the suspension (see "Wall slip correction"), it was measured with the CC25 and CC14 systems. All measurements were repeated three times at $T = 20.0 \pm 0.01$°C following the measurement procedure and calculations presented earlier. For further investigation, the three individual measurements were averaged. Figure 3 shows the exemplary results for the silicon oil AK 5000, which shows a nearly ideal Newtonian behaviour in the observed shear rate

range. This is also valid for the other silicon oil and the suspension. The linear regressions with the corresponding values can be seen in Table 3.

Laboratory results — determination of radius corrections using silicon oil AK 5000

In order to determine the radius corrections, the normalized viscosities were measured for AK 5000 with all systems (see Fig. 4), with the error bars representing the gaussian error. The silicone oil AK 5000 was preferred to the AK 1000 for this investigation, since, due to the higher viscosity, a higher measuring accuracy can be expected. However, as the shear rates up to $\dot{\gamma} = 2s^1$ show some fluctuations, only shear rates larger than $\dot{\gamma} = 2s^1$ will be used for deriving the correction.

All measurements show viscosity values which are lower than the reference viscosity and, as expected, with a greater deviation for the wide grooves. Furthermore, a clear groove depth dependency can be observed for all systems, as the normalized viscosity decreases with increasing groove depth. However, the Newtonian flow behaviour stays unharmed. One can conclude that there is no shear rate dependency of the penetration depth, which is supported by the results obtained by Bauer et al. (Bauer et al. 1995). Therefore, a radius correction was derived for the individual groove depths and widths by averaging over all shear rates larger than $\dot{\gamma} = 2s^1$ (see Fig. 5). The error bars represent the gaussian error.

As to be suspected, Δr increases with increasing groove depth, meaning that the flow penetrates the grooves deeper. This is different from grooves in parallel-plate geometries where a maximum penetration depth could be observed (Pawelczyk et al. 2020). However, the same behaviour might appear for greater groove depths. Nevertheless, some differences can be pointed out between the gap widths. The first thing becoming obvious is the range of the values for Δr. For the narrow grooves, the correction radius is in the range of approximately $37 - 43\mu m$, whereas this range is $83 - 93\mu m$ for the wide grooves. Furthermore, for the narrow grooves, Δr seems to show a linear dependency of the groove depth ($R^2 = 0.9944$). For the wide grooves, this conclusion can only be drawn with certain limitations ($R^2 = 0.945$).

The increase of Δr with increasing groove depth is not surprising. An explanation for the increasing correction factor could be that as the groove depth increases, the fluid experiences less resistance when entering the groove. It is intended to clarify this trend with further investigations in the future but up to now no further prediction is possible. However, whether the penetration depth really increases with increasing groove depth cannot be investigated easily via laboratory measurements and must be considered in more detail via simulations (see "Simulation results").

Application of the radius correction to silicon oils

Figure 6 shows the corrected values for all measurement systems according to Eq. (13) for AK 5000.

As can be seen, the corrected values match the reference viscosity (measured with CC27) with nearly no deviation (see also Table 4).

This is not surprising, as the values for Δr were calculated also using Eq. (13). However, the general purpose of radius corrections is to have a material-independent, but geometry-dependent characteristic value, with which the measured fluids can be corrected. Therefore, it is desirable that the value determined above can also be used for other fluids, which we have already shown for a parallel plate setup (Pawelczyk et al. 2020). In order to prove that correlation for coaxial systems, the obtained correction values for the AK 5000 were also used to correct the AK 1000 measurements (see Fig. 7). The correction values were also applied to suspension measurements (see "Application of the radius correction to silicon oils").

Although the corrected values for AK 1000 do not match the reference viscosity as good as they do for the AK 5000,

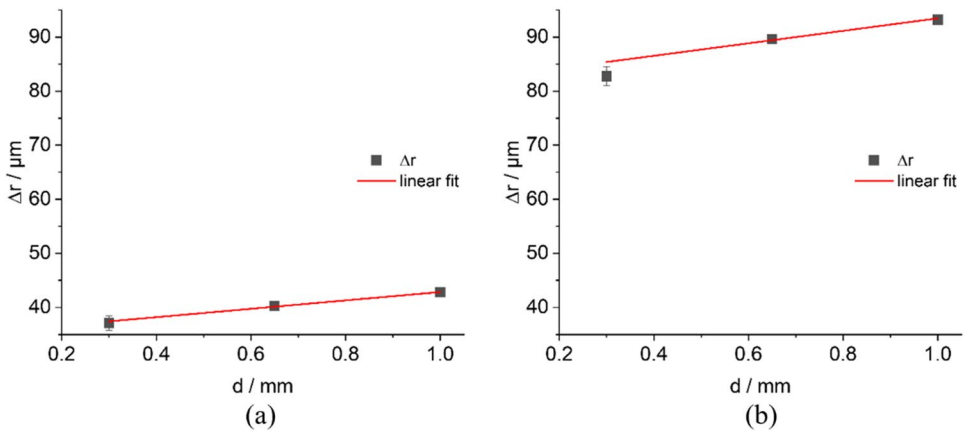

Fig. 5 Radius correction Δr over groove depth d for narrow ($w = 1.1$ mm) groves (**a**) and wide ($w = 2.1$ mm) grooves (**b**)

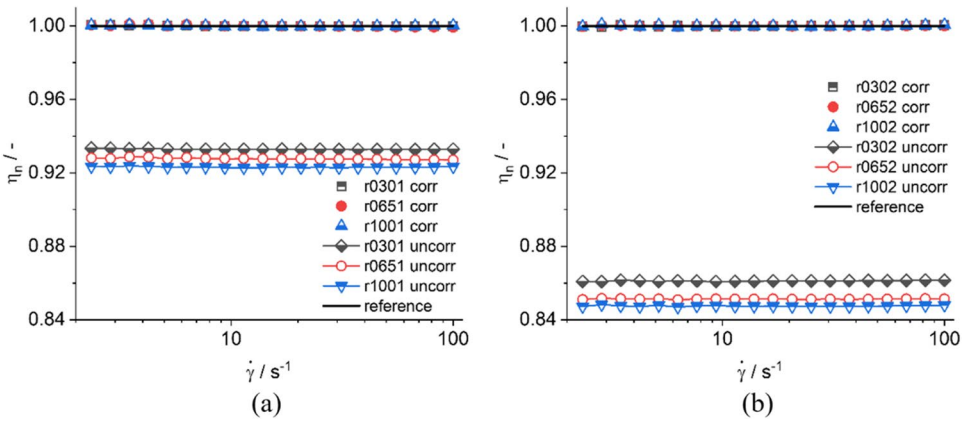

Fig. 6 Corrected and uncorrected normalised viscosities η_n over the shear rate $\dot{\gamma}$ for silicon oil AK 5000 calculated for narrow groves (**a**) and wide grooves (**b**)

Table 4 Averaged deviations over all shear rates of corrected viscosity to reference viscosity for silicon oil AK 5000

Measuring system	Mean deviation/%
r0301	0.00 ± 0.03
r0651	0.00 ± 0.05
r1001	0.00 ± 0.03
r0302	0.00 ± 0.03
r0652	0.00 ± 0.02
r1002	0.00 ± 0.04

the results still look very satisfying, which again is supported by the results obtained by Bauer et al. (Bauer et al. 1995). When taking a closer look at the mean deviations depicted in Table 5, it can be assumed that the correction values Δr are indeed transferable to other materials, provided that they are also Newtonian. As the difference in viscosity between AK 1000 and AK 5000 is not that great, this assumption will be verified in further investigations by using Newtonian fluids with much higher viscosities in the future. Whether this also applies to suspensions with nearly Newtonian flow behaviour is investigated in "Application of the radius correction to suspensions".

Simulation results

For validation purposes, the CC27 reference system was first simulated in 2D at three representative shear rates, $\dot{\gamma} = 5.72\text{s}^1$ (low shear), $\dot{\gamma} = 37.6\text{s}^1$ (middle shear) and $\dot{\gamma} = 82.7\text{s}^1$ (high shear) with a virtual length of $L = 0.3\text{mm}$. To compensate even minor measurement variations, an averaged viscosity over three shear rates in the range of the above-mentioned values was used as input parameter. Given the shear rate and the fluid viscosity, it is possible to calculate the torque on the cup and the bob. As convergence criterion, a constant torque for at least 10,000 iteration steps was defined. Following the equations given in "Theoretical background", it is then

Table 5 Averaged deviations over all shear rates of corrected viscosity to reference viscosity for silicon oil AK 1000 corrected with radius corrections determined for silicon oil AK 5000

Measuring system	Mean deviation/%
r0301	0.05 ± 0.07
r0651	0.34 ± 0.08
r1001	0.27 ± 0.04
r0302	0.33 ± 0.08
r0652	0.36 ± 0.06
r1002	0.37 ± 0.06

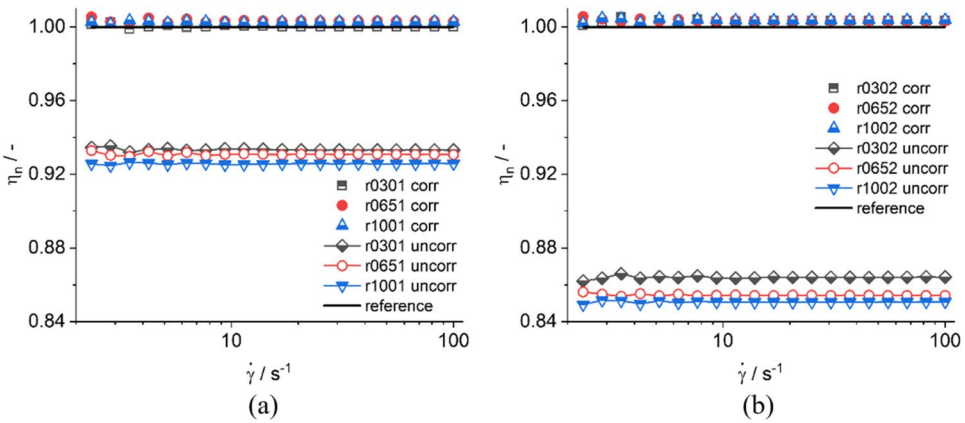

Fig. 7 Corrected and uncorrected normalised viscosities η_n over the shear rate $\dot{\gamma}$ for silicon oil AK 1000 calculated with the radius corrections determined for silicon oil AK 5000 for narrow groves (**a**) and wide grooves (**b**)

Table 6 Reference η_{ref} and simulated η_{sim} viscosity of silicon oil AK 5000 at three different shear rates with the associated deviation

$\dot{\gamma}/s^1$	η_{ref} /Pa · s	η_{sim}/Pa · s	Deviation/%
5.72	5.212	5.210	−0.040
37.6	5.209	5.208	−0.024
82.7	5.200	5.198	−0.024

possible to calculate the shear stress from the torque and the corresponding viscosity which should match the input viscosity if everything is set up correctly. The results are shown in Table 6.

When looking at the deviations, it becomes clear that this approach, including the MRF method, the 2D simulation and the calculation of viscosity, seems appropriate and can be used in the following investigation.

Simulation results — comparison between laboratory and simulation results

The simulations performed for the reference system were also performed for all structured systems with the same initial conditions and convergence criteria. The results are presented in Table 7.

Even though the deviations in viscosity are slightly larger compared to the reference system, they are below 1.5% for all simulations. Therefore, it is possible to calculate the correction factors for similar grooved geometries only via simulation. As the calculation of Δr is viscosity based with a minute deviation, the results are not shown here, since no further insight would be achieved.

Simulation results — investigation of the penetration depth and the flow field via simulation

One of the basic assumptions to derive the radius correction is the even flow penetration of the grooves at the inner and outer cylinders, meaning $\Delta r_i = \Delta r_o = \Delta r$. However, because of the small penetration depth and optical accessibility, it is very complicated to access this experimentally, but a lot easier via simulation.

In this respect, it should be emphasized again that the radius correction is only a correction value and cannot be directly compared with the actual penetration depth of the fluid. While it can be considered an approximation to some extent, it serves more as a relative comparison between the different structures and, what is the main task, as a correction value.

In order to evaluate the relations between Δr_i and Δr_o, some post-processing of the simulation results or the individual cell values, respectively, is necessary. The main

Table 7 Laboratory η_{lab} and simulated η_{sim} viscosity of silicon oil AK 5000 measured and simulated with the structured geometries at three different shear rates with the associated deviation

Low shear —$\dot{\gamma} = 5.72s^1$			
System	η_{lab}/Pa · s	η_{sim}/Pa · s	Deviation/%
r0301	4.863	4.833	0.624
r0651	4.838	4.814	0.498
r1001	4.812	4.811	0.038
r0302	4.488	4.449	0.879
r0652	4.436	4.378	1.319
r1002	4.416	4.355	1.392
Middle shear —$\dot{\gamma} = 37.6s^1$			
System	η_{lab}/Pa · s	η_{sim}/Pa · s	Deviation/%
r0301	4.859	4.830	0.585
r0651	4.831	4.811	0.415
r1001	4.808	4.808	0.000
r0302	4.486	4.446	0.895
r0652	4.434	4.375	1.322
r1002	4.414	4.352	1.395
High shear —$\dot{\gamma} = 82.7s^1$			
System	η_{lab}/Pa · s	η_{sim}/Pa · s	Deviation/%
r0301	4.850	4.821	0.594
r0651	4.820	4.802	0.378
r1001	4.800	4.799	0.029
r0302	4.479	4.438	0.924
r0652	4.427	4.367	1.350
r1002	4.408	4.344	1.449

reason for this is that the actual penetration depth δ of the flow field could only be observed at the outer cylinder, as the flow velocity at the inner cylinder is too high to detect the fluid penetration into the structure, which is much slower. Therefore, a post processing was designed and integrated in a modified solver, which recalculates the velocity field in the measuring gap as follows. All elements in the region $0 < r < r_i$ are seen as a solid state vortex having the radius dependent overlaying velocity $u(r) = r \cdot \omega_i$ with the angular velocity of the inner cylinder ω_i. The overlaying velocity field $u(r)$ in the region $r_i < r < r_o$ is approximated linear with the boundaries $u(r_i) = \omega_i \cdot r_i$ and $u(r_o) = 0$. These overlaying velocity values are subtracted from the calculated velocity values of the cells at the corresponding radii. As all elements laying in the region $r > r_o$ can also be seen theoretically as a solid state vortex, but with an angular velocity of $\omega_o = 0$, no recalculations for these elements need to be conducted. This manipulation emphasizes the areas of interest and enables a direct comparison, that is not dominated by the high velocities of the inner cylinder. Figure 8 illustrates the areas just mentioned, and Fig. 9 shows the comparison between an unmodified and a modified flow field to be analysed further. A vortex-like flow field appears, which indicates how deep the fluid penetrates the structures, since the

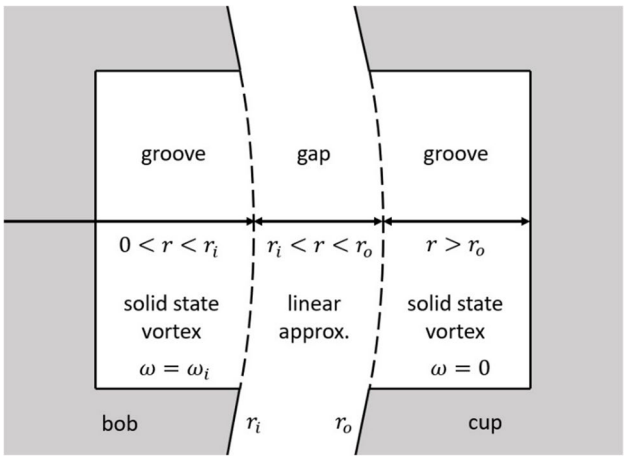

Fig. 8 Schematic visualisation of the regions for recalculating the flow field in the measuring gap

velocities differ maximally from the assumed ideal velocities with no penetration at all. Even though there was no correction in the outer gap, the results differ from the original measurement since the maximum velocity is lower and no longer masks the flow in this area.

An algorithm in MATLAB was written, which calculates the penetration depth δ over the groove width on the basis of a velocity plot in radial direction (see Fig. 10a). Starting from the inner or outer radius, respectively and going into the groove, a circumferential speed of $v_c = 0\mathrm{m/s}$ in the new calculated velocity field was defined as a reference point for calculating the penetration depth, as this point describes the reversal of the flow direction (see Fig. 10a and b). The penetration depth has a maximum in the middle of the groove (angular direction), as it should be expected, and is nearly the same for all inner/outer groove-overlapping situations (see Fig. 11). It is to mention that only a quarter of the measuring system was considered to reduce simulation time making use of the symmetric shape. The values for two directly opposing grooves are given as an example in Fig. 12.

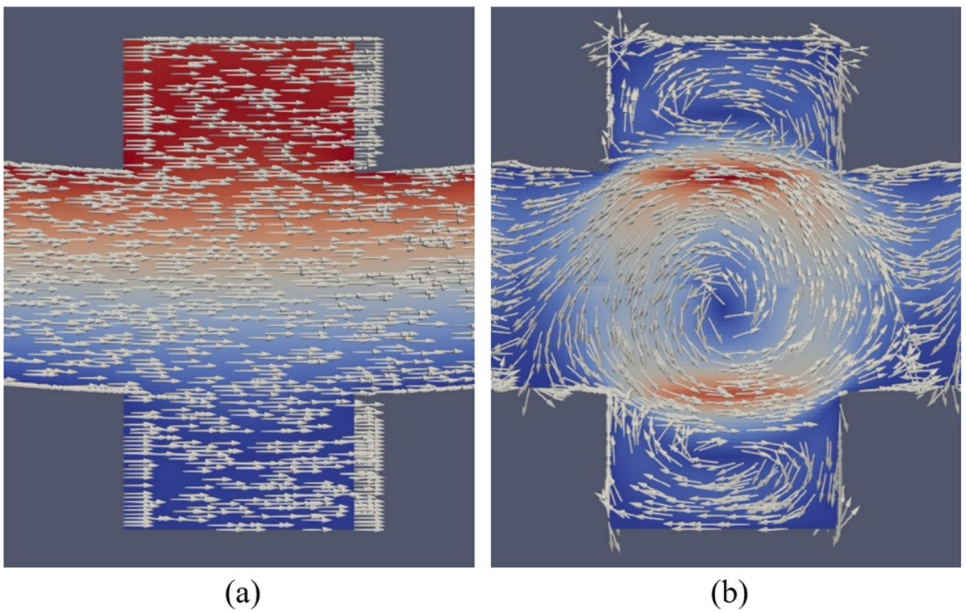

Fig. 9 High shear velocity field with the corresponding vectors in the measuring gap of two opposing grooves of the system r0651 before recalculation (**a**) and after recalculation (**b**) with the new post processing. It must be noted that the scale is different in both depictions, even though the colours and the vector lengths appear to be similar. This has been done for better clarity, since the overall velocity is much lower in figure (**b**)

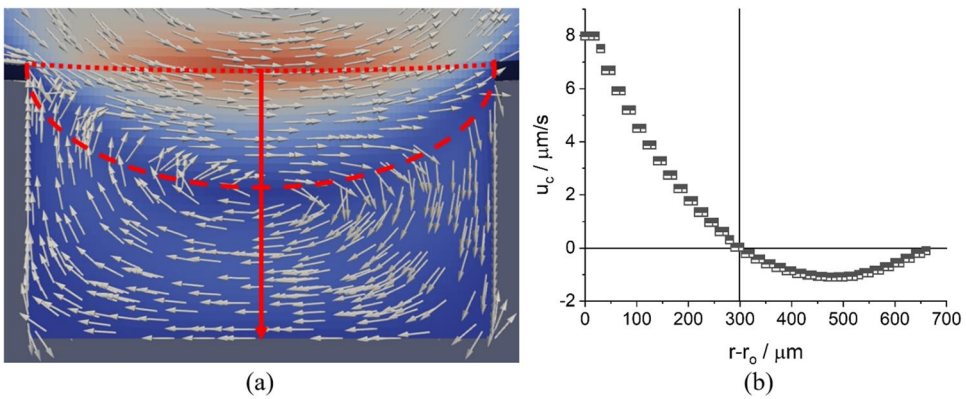

Fig. 10 **a** Schematic visualization for calculating the penetration depth, presented for the r0651 grooves for one position (groove middle) with the outer radius (dotted line), the line for the velocity plot (solid line) from r_o into the groove and the calculated penetration depth (dashed line, schematic illustration); **b** circumferential speed v_c over radius ($0 = r_o$ to end of groove) with marked penetration depth at $v_c = 0$

Table 8 shows the individual averaged penetrations depths for the inner and outer grooves of all systems. To obtain these values, the penetration depths for each individual groove, as presented in Fig. 12, were first averaged over the groove width. This was done for all different overlapping cases (Fig. 11) at the inner and outer cylinders. Then, all these "mean penetration depths" for each individual groove were averaged, to generate only one characteristic parameter for the inner and the outer grooves, respectively. In order to be able to compare the results of the algorithm for the different shear rates more precisely, the first two decimal places are given at this point.

As can be seen in Table 8, the penetration depths do not depend on the shear rate, as only minute deviations occur, which might have their origin in computational accuracy. Therefore, all further discussion will focus on the results of the low shear rate region, but is valid for all regions.

Analysing the penetration depth for the outer and inner grooves, it is obvious that no general conclusion can be drawn, whether δ is greater at the inner cylinder or vice versa. For the narrow grooves the maximum difference (2.08%) is smaller than for the wide grooves (6.57%). Generally, no trend can be seen for both systems. For example, δ is greater at the inner grooves for one system (r0302), but for

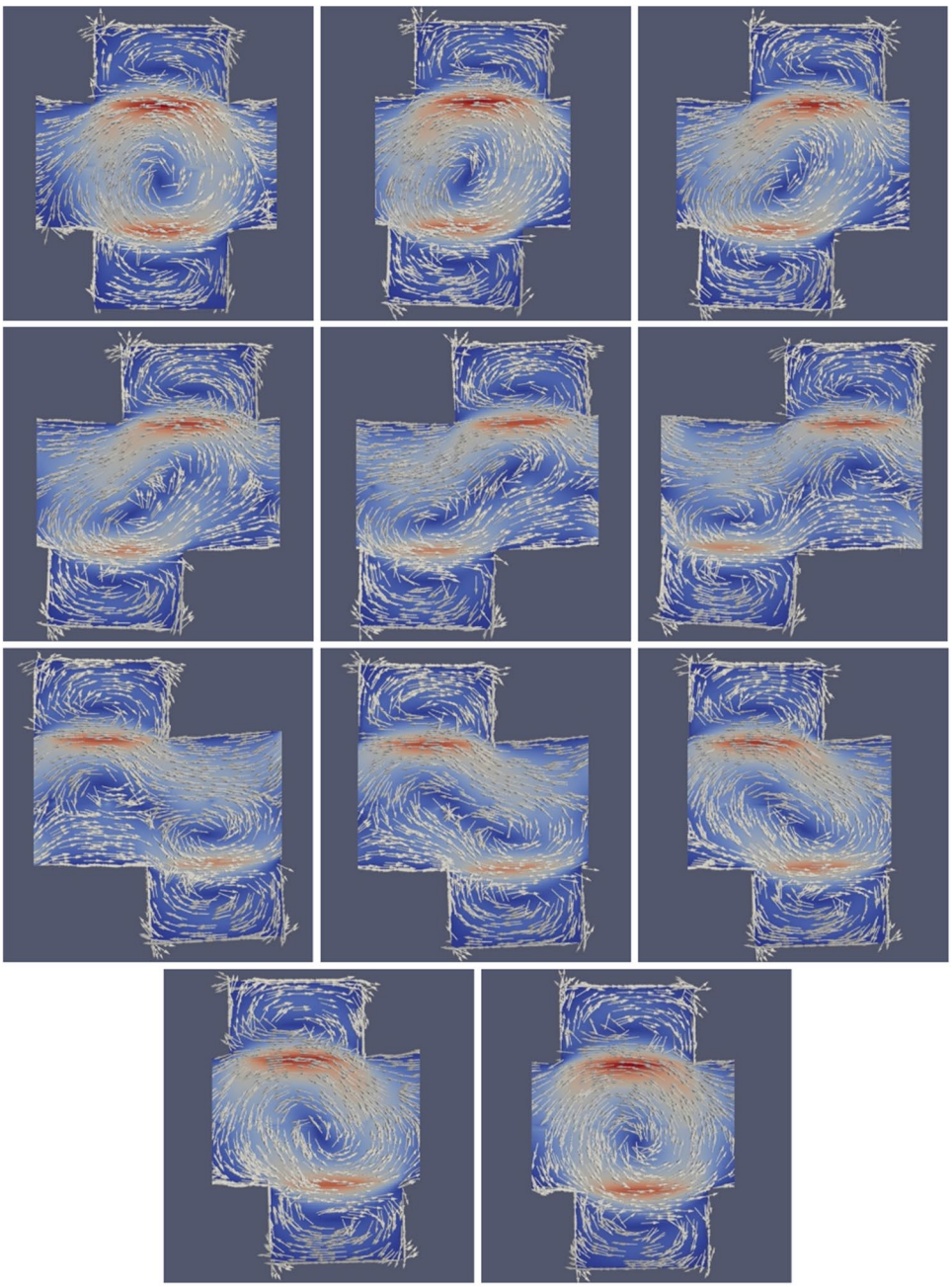

Fig. 11 Different overlapping situations for the modified flow field, exemplary presented for the r0651 geometry

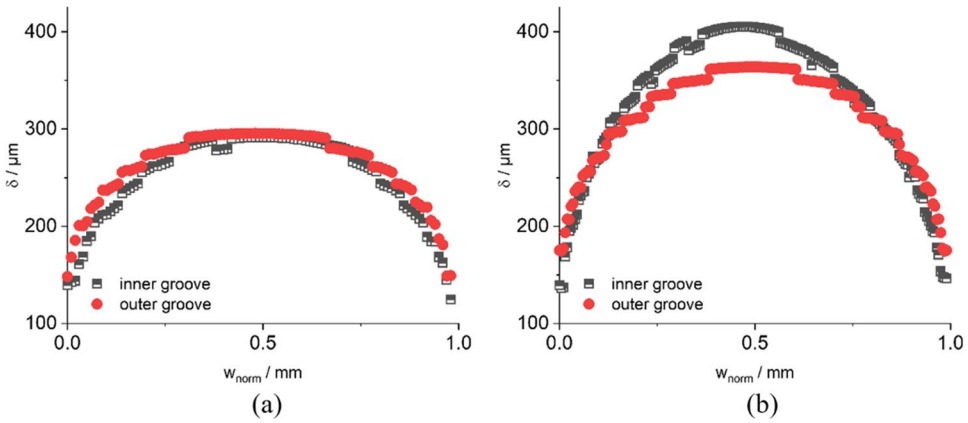

Fig. 12 Penetration depth δ over normalised groove width w_{norm} for the inner and outer grooves calculated for the measuring system r0651 (**a**) and r0652 (*b*) at high shear for two directly opposing grooves

Table 8 Averaged penetration depths δ for all measuring systems at the inner and outer grooves

Narrow	Penetration depth δ inner grooves /μm			Penetration depth δ outer grooves/µm		
$\dot{\gamma}$/s^{1}	r0301	r0651	r1001	r0301	r0651	r1001
5.72	239.92	237.50	266.53	240.36	242.43	266.45
37.6	239.92	237.50	266.48	240.36	242.44	266.48
82.7	239.92	237.50	266.53	240.37	242.44	266.45
Wide	Penetration depth δ inner grooves/µm			Penetration depth δ outer grooves/µm		
$\dot{\gamma}$/s^{1}	r0302	r0652	r1002	r0302	r0652	r1002
5.72	267.12	422.55	404.73	250.66	430.01	430.13
37.6	267.12	422.56	404.74	250.66	430.02	430.13
82.7	267.13	422.57	404.74	250.66	430.03	430.14

another system (r1002), this behaves the other way round. Therefore, the assumption $\Delta r_i \approx \Delta r_o$ seems to be a valid assumption for the small and the wide grooves, meaning the approach presented in Eq. (13) is not only justified, but is also related to the real flow behaviour.

However, looking at the averaged penetration depths (Table 8) reveals no clear trend or correlation. This might be a hint that the state of groove overlapping is important. Therefore, additional investigations analysing the maximum penetration depth, i.e. in the middle of the groove (see Fig. 12), at certain points were carried out, in fact at two opposite grooves (GG), at inner groove opposite outer wall (IGO) and at outer groove opposite inner wall (OGI) (see Table 9). Additionally, since the groove depths differ slightly in the groove middle (see Fig. 2), the ratio of penetration depth to groove depth is listed to obtain more significant information.

The results clearly show that for many systems, the fluid penetrates the whole groove depth. It can also be seen that there is a direct relation between the maximum penetration depth and groove depth, as with increasing groove depth the maximum penetration depth increases, too. This also applies to the groove width, since the same relationship exists. However, this matches the assumptions made in "Simulation results — comparison between laboratory and simulation results" of higher penetration depths with increasing groove depths and widths due to the lower resistance of the cylinder walls. Taking a closer look, it stands out that no great deviations exist between inner and outer grooves, except for $d_{GG,o}/d_o$ for the system r1002, while the reason for this exception remains unknown. When comparing the penetration depths for inner and outer grooves for those systems, where the fluid does not penetrate the entire groove (r0651 and r1001), it can also be seen that here, too, the penetration depths for inner and outer grooves are in a similar range with only small deviations, which again supports the assumption of $\Delta r_i = \Delta r_o$.

Application of the radius correction to a suspension

Our investigation clearly shows that the determination of the radius correction values can be greatly simplified by simulations. However, the use of structured systems is only necessary for wall slip materials such as suspensions. Therefore, it is of high interest, if the radius corrections determined for the silicon oil AK 5000 are also applicable to suspensions within an acceptable deviation. To this end, a 21.23vol% suspension of silicon oil AK 5000 and Spheromers® CA40 was prepared and corrected for slip using the described methods (see "Wall slip correction")

Table 9 Maximum penetration depths δ in the groove middle for different cases with according ratio of penetration depth δ to groove depth d

Inner grooves		Opposite grooves		Inner groove opposite outer wall	
System	d_i/µm	$\delta_{GG,i}$/µm	$\delta_{GG,i}/d_i$	δ_{IGO}/µm	δ_{IGO}/d_i
r0301	300	299	0.997	300	1.000
r0651	650	293	0.451	261	0.402
r1001	1000	333	0.333	302	0.302
r0302	300	299	0.997	300	1.000
r0652	650	650	1.000	405	0.623
r1002	1000	588	0.588	386	0.386
Outer grooves		Opposite grooves		Outer groove opposite inner wall	
System	d_o/µm	$\delta_{GG,o}$/µm	$\delta_{GG,o}/d_o$	δ_{OGI}/µm	δ_{OGI}/d_o
r0301	289	288	0.997	288	0.997
r0651	639	299	0.468	255	0.399
r1001	989	328	0.332	288	0.291
r0302	259	258	0.996	258	0.996
r0652	609	608	0.998	368	0.604
r1002	959	663	0.691	353	0.368

while measured with smooth surface systems. The true viscosity η_{true} is illustrated in Fig. 13, with the error bars representing the gaussian error in case of η_{true} and the standard deviation in case of η_a.

As expected, the uncorrected viscosity values are slightly lower than the corrected viscosity, indicating wall slip. However, it is quite significant, that the uncorrected values show an apparent slightly shear thinning behaviour, whereas the corrected values indicate a Newtonian flow behaviour with a mean viscosity of $\eta = 11.369 \pm 0.017\text{Pa} \cdot \text{s}$. The shear thinning effect could be attributed to a higher slip-velocity at high shear rates, showing that wall slip may also lead to a false conclusion regarding the flow behaviour. However, a general shear-thinning behaviour of the suspension could be excluded, since not only the presented values, but also previous measurements conducted with a parallel-plate system and according wall slip correction showed a Newtonian flow behaviour (Pawelczyk et al. 2020).

After the true viscosity was determined as a reference, the suspensions were measured with the structured systems, and the radius correction values determined for pure silicon oil AK 5000 were applied. Figure 14 shows the uncorrected and the corrected normalised viscosities together with the reference viscosity. Again, due to measuring errors in the very low shear rate range, only the values above $\dot{\gamma} = 2\text{s}^1$ are considered. The slight tendency to apparent shear-thickening, especially for the system r1001 can be attributed to measurement errors due to minimal dimensional inaccuracies of the measuring systems. However, as this behaviour is not strongly pronounced, it will be neglected in the further course of investigating the transferability of the radius corrections.

The good agreement of the corrected values with the reference curve again strengthens the fact that the Δr is

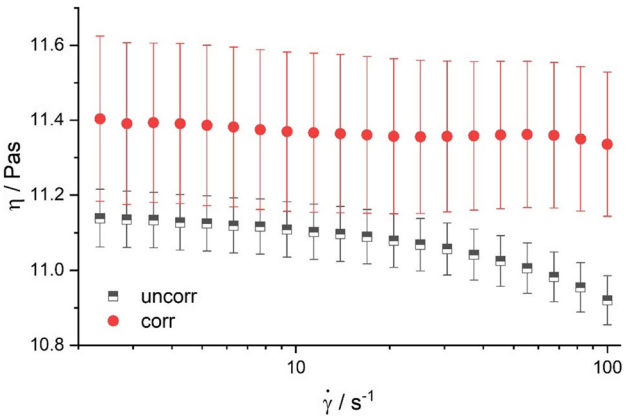

Fig. 13 Uncorrected and wall-slip-corrected viscosity over the shear rate for a suspension made of silicon oil AK 5000 and 21.23vol% Spheromers® CA40 measured with smooth bob und cup systems

transferable and measurements with structured geometries are possible for suspensions. This is due to the fact that the corrected normalised viscosites differ from the reference values by a maximum deviation of only 3.5% (measuring system r1001) (see Table 10).

When looking at these deviations, it should always be kept in mind that the wall slip corrections were performed using two self-manufactured systems. Therefore, slight deviations may be explained by inaccuracies of the measuring systems and the flow behaviour. Nevertheless, these deviations are within a normal measurement uncertainty, so that, including the results for the silicon oil AK 1000, the conclusion can be drawn that the radius corrections can be generally applied to Newtonian fluids. However, further investigations with Newtonian fluids would be useful to verify this assumption.

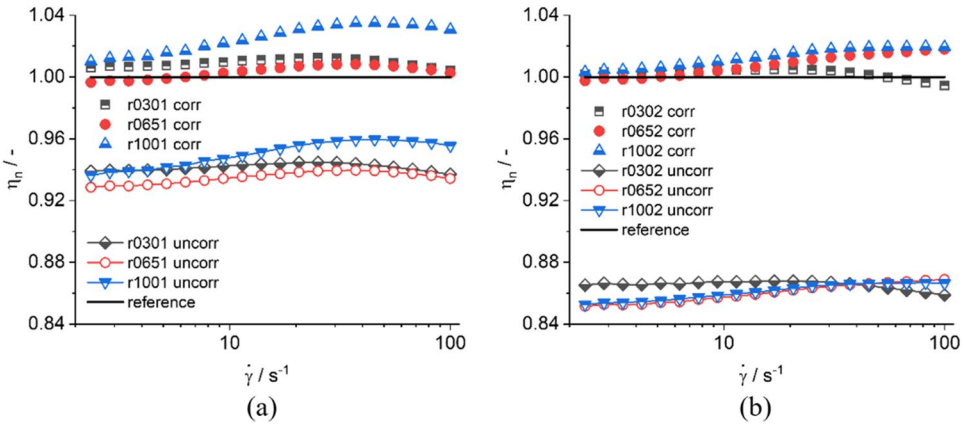

Fig. 14 Corrected and uncorrected normalised viscosites η_n over the shear rate $\dot{\gamma}$ for a suspension (AK 5000 with 21.23vol% Spheromers® CA40 particles) calculated with the radius corrections determined for silicon oil AK 5000 for narrow groves (**a**) and wide grooves (**b**)

Table 10 Averaged deviations over all shear rates of corrected viscosity to reference viscosity for a suspension (AK 5000 + 21.23vol% Spheromers® CA40 particles) corrected with radius corrections determined for silicon oil AK 5000

Measuring system	Mean deviation/%
r0301	0.899 ± 0.247
r0651	0.327 ± 0.404
r1001	2.511 ± 0.891
r0302	0.509 ± 0.292
r0652	0.754 ± 0.707
r1002	1.280 ± 0.606

In this context, it is to mention that the same research was conducted with shear thinning fluids, but no general solution could be found, as the correction values seem to be dependent not only on the shear rate but also on the extent of the shear thinning flow behaviour. Therefore, these investigations are important and will be pursued in the future.

Conclusions

The general approach for measuring suspensions, which are prone to wall slip, is to use structured geometries without recalculating the effective radius for the determination of rheological properties. However, our investigation clearly shows that structured geometries lead to false values with much lower viscosities, which need to be corrected in any case.

We are able to show that the effective radius can be corrected with a geometry-dependent, but material- and shear rate-independent correction value Δr, provided Newtonian fluids measured and the assumption of an equally penetrating fluid at the inner and outer cylinders is made, meaning $\Delta r_i = \Delta r_o = \Delta r$. This assumption could be backed up via simulative results. The generality of the correction factor was shown by determining the mean radius corrections using a reference fluid, in this case the silicon oil AK 5000, and using these values to correct other Newtonian fluids, namely silicon oil AK 1000 and a suspension consisting of silicon oil AK 5000 and 21.23vol% Spheromers® CA40 particles. While the application of the correction values to AK 1000 lead to very small deviations of only $0.05 - 0.37\%$, the deviations for the suspension were slightly higher with $0.327 - 2.511\%$. For some systems, especially for the system r1001, the values improved by only a small percentage compared to the uncorrected values, so that a correction does not seem necessary. However, this is still a quite promising result, especially considering that the investigation of the suspension was based on self-manufactured measurement systems and other measurements could be enhanced significantly. It is very likely that this purely geometrical correction works for all Newtonian fluids. However, it has to be proven for much higher viscosities in the future.

Since both, the fabrication of structured systems and the measurement of the material in the laboratory, are very time-consuming and costly, a simulative approach to determine the radius corrections was investigated. The CFD results lead to two conclusions. On the one hand, the simulation is able to reproduce the laboratory results with high precision. On the other hand, it could be shown that the assumption of $\Delta r_i = \Delta r_o = \Delta r$ to correct the apparent viscosity measured with structured systems is justified, since the averaged penetration depths between inner and outer cylinders only differed little, if at all. Therefore, the use of a simulative approach for determining the radius correction should be preferred in any case.

Funding Open Access funding enabled and organized by Projekt DEAL.

Data availability If desired the raw data will be given to any researcher on a reasonable request.

References

Ahuja A, Singh A (2009) Slip velocity of concentrated suspensions in Couette flow. J Rheol 53(6):1461–1485. https://doi.org/10.1122/1.3213090

Ballesta P, Petekidis G, Isa L, Poon WCK, Besseling R (2012) Wall slip and flow of concentrated hard-sphere colloidal suspensions. J Rheol 56(5):1005–1037. https://doi.org/10.1122/1.4719775

Banfill PFG (1991) Rheology of fresh cement and concrete. Taylor & Francis, Abingdon

Barnes HA (1995) A review of the slip (wall depletion) of polymer solutions, emulsions and particle suspensions in viscometers: its cause, character, and cure. J Non-Newtonian Fluid Mech 56(3):221–251. https://doi.org/10.1016/0377-0257(94)01282-M

Bauer H, Bse N, Stern P (1995) Viscoplastic flow and shear thickening in concentrated diblock copolymer solutions. Colloid Polym Sci 273(5):480–489. https://doi.org/10.1007/bf00656893

Beavers GS, Joseph DD (1967) Boundary conditions at a naturally permeable wall. J Fluid Mech 30(1):197–207. https://doi.org/10.1017/S0022112067001375

Besseling R, Isa L, Ballesta P, Petekidis G, Cates ME, Poon WCK (2010) Shear banding and flow-concentration coupling in colloidal glasses. Phys Rev Lett 105(26):268301. https://doi.org/10.1103/PhysRevLett.105.268301

Carotenuto C, Minale M (2013) On the use of rough geometries in rheometry. J Non-Newtonian Fluid Mech 198:39–47. https://doi.org/10.1016/j.jnnfm.2013.04.004

Carotenuto C, Vananroye A, Vermant J, Minale M (2015) Predicting the apparent wall slip when using roughened geometries: a porous medium approach. J Rheol 59(5):1131–1149. https://doi.org/10.1122/1.4923405

Cloitre M, Bonnecaze RT (2017) A review on wall slip in high solid dispersions. Rheol Acta 56(3):283–305. https://doi.org/10.1007/s00397-017-1002-7

Fincke A, Heinz W (1961) Zur Bestimmung der Fließgrenze grobdisperser Systeme. Rheol Acta 1(4–6):530–538. https://doi.org/10.1007/bf01989114

Giesekus H, Langer G (1977) Die Bestimmung der wahren Fließkurven nicht-newtonscher Flüssigkeiten und plastischer Stoffe mit der Methode der repräsentativen Viskosität. Rheol Acta 16(1):1–22. https://doi.org/10.1007/BF01516925

Granick S, Zhu Y, Lee H (2003) Slippery questions about complex fluids flowing past solids. Nat Mater 2(4):221–227. https://doi.org/10.1038/nmat854

Haase AS, Wood JA, Sprakel LMJ, Lammertink RGH (2017) Inelastic non-Newtonian flow over heterogeneously slippery surfaces. Phys Rev E 95(2–1):23105. https://doi.org/10.1103/PhysRevE.95.023105

Jesinghausen S, Weiffen R, Schmid H-J (2016) Direct measurement of wall slip and slip layer thickness of non-Brownian hard-sphere suspensions in rectangular channel flows. Exp Fluids 57(9):159. https://doi.org/10.1007/s00348-016-2241-6

Kalyon DM (2005) Apparent slip and viscoplasticity of concentrated suspensions. J Rheol 49(3):621–640. https://doi.org/10.1122/1.1879043

Kiljański T (1989) A method for correction of the wall-slip effect in a Couette rheometer. Rheol Acta 28(1):61–64. https://doi.org/10.1007/bf01354770

Korhonen M, Mohtaschemi M, Puisto A, Illa X, Alava MJ (2015) Apparent wall slip in non-Brownian hard-sphere suspensions. Eur Phys J E Soft matter 38(5):129. https://doi.org/10.1140/epje/i2015-15046-y

Krieger IM, Elrod H (1953) Direct determination of the flow curves of non-Newtonian fluids. II. Shearing rate in the concentric cylinder viscometer. J Appl Phys 24(2):134–136. https://doi.org/10.1063/1.1721226

Macosko CW (1994) Rheology. Principles, measurements and applications by Christopher W. Macosko. Chichester: Wiley-VCH (Advances in interfacial engineering series)

Mezger T (2012) Das Rheologie-Handbuch. Für Anwender von Rotations- und Oszillations-Rheometern. 4. Aufl. Hannover: Vincentz Network (Farbe und Lack Edition)

Minale M (2014) Momentum transfer within a porous medium. II. Stress boundary condition. Phys Fluids 26(12):123102. https://doi.org/10.1063/1.4902956

Minale Mario (2016) Modelling the flow of a second order fluid through and over a porous medium using the volume averages. II. The stress boundary condition. Phys Fluids 28(2):23103. https://doi.org/10.1063/1.4941576

Mooney M (1931) Explicit formulas for slip and fluidity. J Rheol 2(2):210–222. https://doi.org/10.1122/1.2116364

Neale G, Nader W (1974) Practical significance of brinkman's extension of Darcy's law: coupled parallel flows within a channel and a bounding porous medium. Can J Chem Eng 52(4):475–478. https://doi.org/10.1002/cjce.5450520407

Nickerson CS, Kornfield JA (2005) A "cleat" geometry for suppressing wall slip. J Rheol 49(4):865–874. https://doi.org/10.1122/1.1917846

Paduano LP, Schweizer T, Carotenuto C, Vermant J, Minale M (2019) Rough geometries with viscoelastic Boger fluids: predicting the apparent wall slip with a porous medium approach. J Rheol 63(4):569–582. https://doi.org/10.1122/1.5093288

Paduano LP, Caserta S, Minale M, Carotenuto C (2018) Rheological tests with a Boger fluid and a rough geometry. In. 9TH International conference on "Times of Polymers and Composites": from aerospace to nanotechnology. Ischia, Italy, 17–21 June 2018: Author(s) (AIP Conference Proceedings), p. 20095

Pahl M, Gleißle W, Laun H-M (1991) Praktische Rheologie der Kunststoffe und Elastomere. VDI-Verlag (Kunstsofftechnik), Düsseldorf

Pawelczyk S, Kniepkamp M, Jesinghausen S, Schmid H-J (2020) Absolute rheological measurements of model suspensions: influence and correction of wall slip prevention measures. Materials (Basel, Switzerland) 13 (2). DOI: https://doi.org/10.3390/ma13020467

Schümmer P (1970) Zur Darstellung der Durchflußcharakteristik, viskoelastischer Flüssigkeiten in Rohrleitungen. Chemie Ingenieur Technik 42(19):1239. https://doi.org/10.1002/cite.330421916

Yilmazer U, Kalyon DM (1989) Slip effects in capillary and parallel disk torsional flows of highly filled suspensions. J Rheol 33(8):1197–1212. https://doi.org/10.1122/1.550049

Yoshimura A, Prud'homme, Robert K (1988) Wall slip corrections for couette and parallel disk viscometers. J Rheol 32(1):53–67. https://doi.org/10.1122/1.549963

Zhu Y, Granick S (2002) Limits of the hydrodynamic no-slip boundary condition. Phys Rev Lett 88(10):106102. https://doi.org/10.1103/PhysRevLett.88.106102